ELSEVIER

Journal of Alloys and Compounds 216 (1994) 149–154

Journal of ALLOYS AND COMPOUNDS

Intermetallic compounds formed by electrodeposition of indium on bismuth

Stefano Canegallo, Vassilis Demeneopoulos*, Luisa Peraldo Bicelli, Giovanni Serravalle

Dipartimento di Chimica Fisica Applicata del Politecnico, Centro di Studio sui Processi Elettrodici del CNR, Piazza L. da Vinci, 32, 20133 Milan, Italy

Received 2 May 1994

Abstract

Indium electrodeposition on bismuth cathodes at constant current density and room temperature gives rise to the formation of three intermetallic compounds owing to indium diffusion and reaction inside the electrode. The mechanism of this process has been investigated by scanning electron microscopy, energy-dispersive spectrometry and X-ray diffraction, analysing the morphology, composition and structure of the deposit surface and cross-section. The intermetallic compounds are In_2Bi, In_5Bi_3 and InBi, the latter being the unique compound at the end of the analysed time-scale (1500 h), while In_5Bi_3 never emerged on the electrode surface.

Keywords: Electrodeposition; Indium; Bismuth; Intermetallic compounds

1. Introduction

In two previous papers [1,2] we showed that the plating of indium on bismuth cathodes at room temperature leads to the formation of intermetallic compounds (In_2Bi and InBi) since In diffusion inside the Bi substrate is fast at room temperature.

No other paper has been published on this subject since yet, as only studies on codeposition of In and Bi have been reported. However, these papers are scarce [3]. Sadana and Wang [4,5] showed that In–Bi alloys can be obtained from aqueous baths containing diethylenetriamine pentaacetate complexes of the two metals. Bi–In alloys containing up to 90 wt.% In were deposited by varying bath composition and current density. The X-ray analysis of the original and annealed deposits showed the existence of two intermediate phases. The first was InBi while the second occurred at a much lower Bi content than required for In_2Bi (the phase expected according to the phase diagram) and was assumed to be In_3Bi. Interestingly though, the structure and the lattice parameters of this new phase were the same as those reported for In_2Bi [4]. Recently, Bi–In alloys have been electrodeposited from a bath based on Trilon B containing Bi and In nitrates [6]. Little attention has also been given to In electroplating on foreign metal substrates different from Bi to prepare In alloys or/and intermetallic compounds. Hobson and Leidheiser [7] studied the rate of formation of InSb both thermally at the In/Sb interface at 100 °C and electrochemically by In potentiostatic deposition on Sb and subsequent immersion of the sample in boiling water. They observed that in the last case, the diffusion coefficient of In in InSb (around 10^{-16} m^2 s^{-1}) was at least two orders of magnitude greater than during the thermal synthesis.

The present interest in In–Bi intermetallic compounds for electronic purposes (InBi and In_2Bi are semiconductors, while In_5Bi_3 is a superconductor at 3.38 K) and the availability of more accurate techniques and instrumentation prompted us to deepen our previous research [1,2] with the aim of better defining the composition changes at the sample surface. Indeed, as we will see below, we succeeded in outlining the In diffusion process into the electrode and identified a third intermetallic compound (In_5Bi_3), in addition to In_2Bi and InBi. Such a compound never emerged on

*Present address: Department of Chemical Engineering, Section (III): Material Science, National Technical University, 9 Iroon Polytechniou Road, Zografou 157 73, Athens, Greece.

SSDI 0925-8388(94)01262-G

the electrode surface and, therefore, could not be observed during the electrochemical measurements.

2. Experimental details

The Bi electrode (a cylinder of 16 mm diameter and 20 mm long) was prepared by melting Bi (99.9995% Fluka) and its working area by polishing its surface with silicon carbide paper. The electrochemical cell (Teflon) was of the vertical type with the working Bi electrode on the bottom. The anode was of In (99.999% Fluka). An In wire was used as the reference electrode. It was inserted in a Luggin glass capillary of 1 mm diameter filled with the electrolytic solution and positioned at a distance of 5 mm from the electrode surface. The electrolyte was an aqueous solution of $InCl_3$ (0.67N, pH 1.3). The cell was connected to a power potentiostat-galvanostat (555/B Amel) always operating in galvanostatic conditions. The cell voltage was measured with a precision electrometer (668/RM Amel) and recorded on paper (868 Amel). The potential of the Bi electrode vs. In was measured, during and after electrodeposition, with a digital multimeter (755i Yokogawa) and stored with a fixed frequency on a magnetic medium, thus allowing the numerical post-processing of the data with the aid of a personal computer. Eleven runs were carried out at current densities from 2.4 to 21.4 A m^{-2} and deposition time from 1.2 to 8.3 h, repeating each run several times. The deposited In quantity ranged from 20.4 to 91.7 g m^{-2}, and the corresponding thickness (determined coulometrically taking a current efficiency of 100%, a density of 7.286 g cm^{-3}, and the geometrical area of the electrode) from 2.8 to 12.6 μm. All measurements were performed at 25 °C.

A thin slice (1–2 mm) of the electrode was cut after each run to investigate the deposit properties. The morphology and composition of the deposit surface and cross-section were investigated by scanning electron microscopy (SEM) and energy-dispersive spectrometry (EDS) (Stereoscan 360, Cambridge Instrument and AN10/25-Link). The samples were dipped in liquid nitrogen for a few seconds and broken to reveal their cross-section. The electrode structure before and after In electrodeposition was determined by X-ray diffractometry (PW7010, Philips, Cu Kα).

3. Results and discussion

3.1. Electrodeposition and deposits characterisation

It is worth recalling [8,9] that In exhibits an electrochemical behaviour practically reversible on both the cathodic and anodic side. Increasing the current density, anomalies may be observed on the cathodic side, particularly in indium sulfate baths. They are always associated with a strong increase of the overvoltage and a decrease of the current efficiency due to hydrogen evolution. Experimental conditions (electrolyte composition, pH, current density, etc.) have therefore been selected in which such a parasitic process does not occur. Hence, the deposited In quantity was estimated from the electric charge passed through the system according to the reaction

$$In^{3+} + 3e^- = In$$

Also, the presence of In^+ ions (due to the metal–solution equilibrium) could be neglected from the coulometric point of view.

Typical galvanostatic curves at 2.4 and 14.3 A m^{-2} are shown in Fig. 1(a) and 1(b), respectively (full curves). During these measurements, the circuit was periodically opened for about 30 s to monitor the equilibrium potential of the cathode, and thus the chemical composition of the electrode surface (upper dots). The voltage values under current were affected by a small error due to ohmic drop (high conductivity of the electrolyte and not too high current densities). This was of no concern to us, since only open-circuit data were quantitatively analysed.

At the lowest current density (Fig. 1(a)), the cathode potential vs. In regularly decreased though never reaching the conditions for the formation of pure In. In this case, the open-circuit voltage showed an extended plateau due to the presence of InBi on the electrode surface, in agreement with X-ray results. At a higher

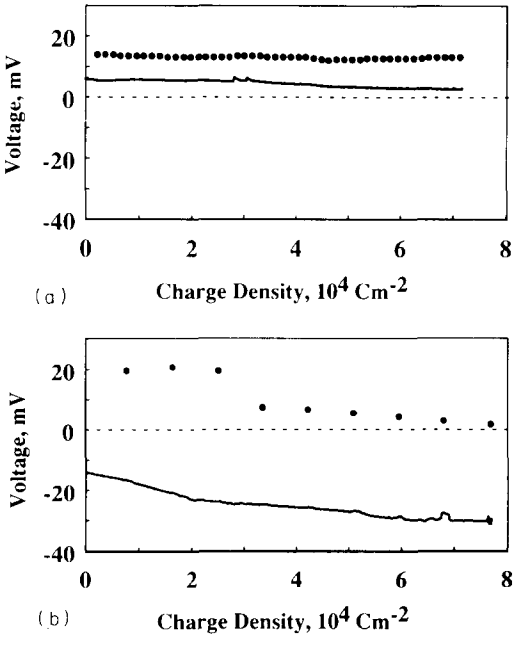

Fig. 1. Cathode potential vs. In in closed-circuit (continuous line) and open-circuit (dots) conditions as a function of the charge circulating during In electrodeposition at (a) 2.4 and (b) 14.3 A m^{-2}.

current density (Fig. 1(b)), the voltage decrease was even more evident. Three quasi-plateaus around 20, 5 and 0 mV were noted on the open-circuit curve. Thermodynamic calculations showed that they were due to InBi, In_2Bi and In. This was confirmed by structural investigation. Tests carried out at low current densities for a short time never reached the zero voltage whereas those at the highest current density (21.4 A m^{-2}) revealed the plateau at 0 mV, only.

The results of the SEM–EDS microanalysis of the deposits agreed with the electrochemical and structural ones. They evidenced once more the strict correlation between the composition of the electrode surface and the electrodeposition conditions.

3.2. Time evolution after deposition

3.2.1. Electrochemical results

Special attention was devoted to changes in the electrode potential after In electrodeposition to obtain information on those in the composition of the electrode surface.

As shown in Fig. 2, a double transition occurs in most cases, since In, and In_2Bi as well, are not stable on the electrode surface. Thus, in Fig. 2(a), curve B presents an extended plateau whose value corresponds to In_2Bi followed by a voltage increase up to the typical value of InBi, whereas curve A (due to a thinner deposit obtained at the same current density as curve B) has a faster evolution showing the plateau of InBi, only.

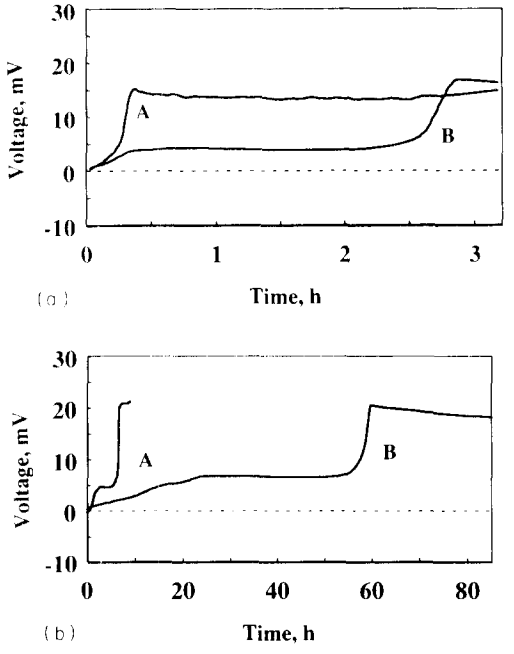

Fig. 2. Time dependence of the cathode potential vs. In after In electrodeposition: (a) at 11.9 A m^{-2} for 1.2 h (curve A) and 1.8 h (curve B); (b) at 21.4 A m^{-2} for 1.5 h (curve A) and 3 h (curve B).

Similar arguments apply to the curves in Figs. 2(b) due to deposits obtained at a higher current density. Note the greater time-scale in Fig. 2(b) in comparison to Fig. 2(a).

3.2.2. SEM and EDS results (sample surface)

In all cases where the final electrode potential vs. In was equal to zero, isolated In microcrystals were observed on the sample surface immediately after electrodeposition (Fig. 3(a)). These microcrystals emptied out and collapsed on the sample surface (just as though In was being diffused into the bulk of the electrode) as clearly shown in Fig. 3(b)–(d) taken 21 to 145 h after electrodeposition. The smaller the deposited In quantity, the faster was such time evolution.

Simultaneously with the SEM observations, the In surface concentration was analysed by EDS as a function of time. Here and in the following, we mainly refer to deposits typically obtained at 21.4 A m^{-2} for 3 h. Their thickness was not smaller than 12.58 μm (the theoretical value of pure In) while the emission depth of the backscattered electrons was smaller than 1 μm. Thus, we mainly investigated the deposit surface. Since the latter was strongly heterogeneous (Fig. 3(a)), we analysed a sufficiently large area to get the medium value. The results are reported in Fig. 4. Because of the time necessary to perform the analysis, the In surface concentration was initially not higher than 90 wt.% and then regularly decreased to the value of 35.6 wt.%, very close to that of InBi (35.46 wt.%).

3.2.3. SEM and EDS results (sample cross-section)

Deeper details on changes in the morphology and composition of the deposits were obtained by analysing their inner structure as a function of time. In this case, the whole modified layer of the electrode was explored. As stated in Section 2, the samples were cut after immersion in liquid nitrogen for a few seconds. Typical results are shown in Fig. 5, where the In-line profile, scanned along the white line in the micrographs, is reported below each SEM image. The results show that the deposit has a multilayered structure and contains three intermetallic compounds: In_2Bi, In_5Bi_3 and InBi. However, only one of them is present inside each layer, and their sequence from the surface to the bulk is In_2Bi–In_5Bi_3–InBi. This is particularly evident, for example, in Fig. 5(c), by comparing the ratio between the height of the peaks with the ratio between the theoretical In concentration in the various intermetallic compounds. In all cases, the unique, homogeneous layer at the end of the experiment (lasting 1500 h) had the InBi composition.

It is noteworthy that this is the first time that In_5Bi_3 has been observed in In electrodeposits on Bi. However, no additional plateau was noticed in the discharge curves, a clear indication that In_5Bi_3 never emerged

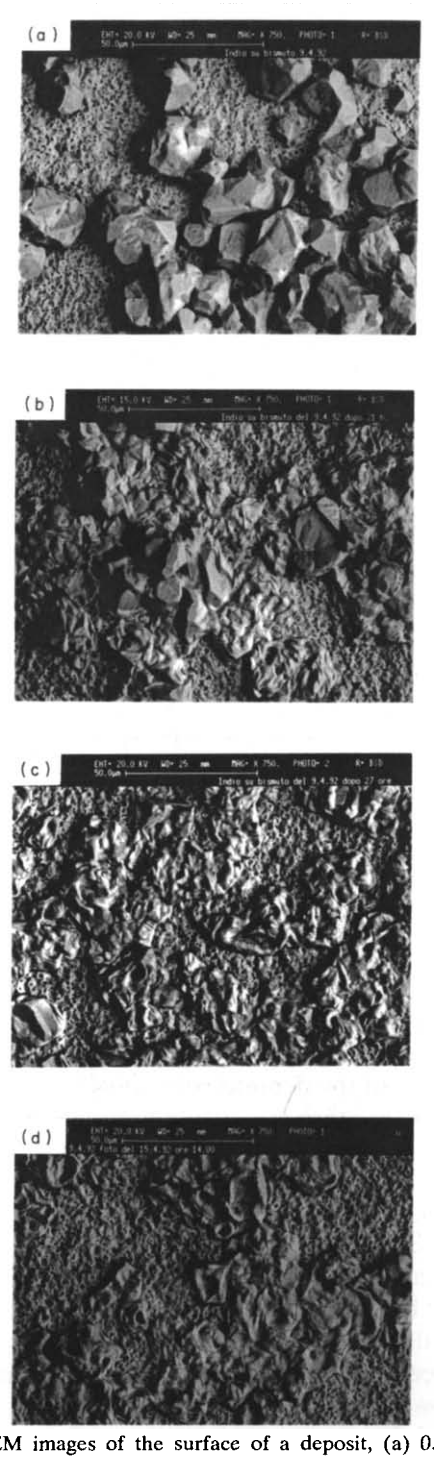

Fig. 3. SEM images of the surface of a deposit, (a) 0.5 h, (b) 21 h, (c) 27.2 h and (d) 145 h after In electrodeposition at 21.4 A m^{-2} for 3 h.

on the electrode surface (for direct experimental evidence, see below).

To emphasize the difficulty in observing In_5Bi_3 when other In–Bi intermetallic alloys are present, note that only in 1967 [10] was In_5Bi_3 recognized in a revised In–Bi equilibrium phase diagram, in addition to In_2Bi and InBi [11,12]. Recently, the presence of In_5Bi_3 in

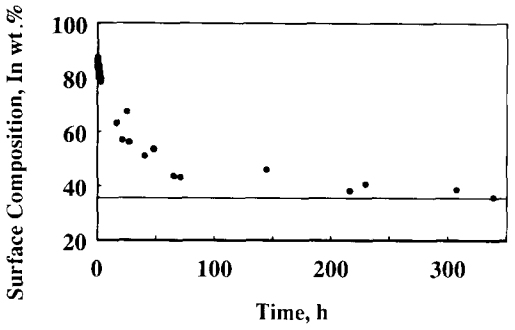

Fig. 4. Indium surface weight percentage as a function of time after In electrodeposition at 21.4 A m^{-2} for 3 h. The continuous line shows the composition of InBi.

such a phase diagram has been confirmed by thermodynamic calculations [13].

By SEM–EDS analysis, we also determined the thickness of each layer and the cumulative thickness of the deposit as a function of time (Fig. 6). Owing to the limited reproducibility, at least ten measurements were carried out on each of the three micrographs taken from different regions of the sample section. However, a significant value of the In layer thickness could not be obtained because of the irregular distribution of In microcrystals on the electrode surface, as already underlined. After 0.7 h, the total deposit thickness was 15.59 ± 1.52 μm, i.e. in between that of In (12.58 μm) and InBi (28.69 μm, assuming a density of 9.012 g cm^{-3}), while after 1193.2 h, it was 25.3 ± 0.7 μm.

Fig. 6 shows the trend of the process of diffusion and reaction, clearly evidencing that In_5Bi_3 never emerges on the electrode surface. So, after a certain time (around 100 h in our example) the previous sequence of the intermetallic compounds (In_2Bi–In_5Bi_3–InBi) has to be modified in In_2Bi–InBi, the latter being the unique compound at the end of the analysed time-scale.

3.2.4. X-ray results

The original Bi and In electrodes showed a perfect correspondence between their X-ray diffraction peaks and those reported in the ASTM tables [14]. The diffraction pattern of the Bi cathode 10 h after In electrodeposition (at 21.4 A m^{-2} for 3 h) are compared in Fig. 7 with the schematic peaks [14] of Bi, In and the intermetallic compounds. Notwithstanding the overlapping of several peaks, it is possible to find at least one characteristic peak to identify each metal or compound, as shown by the dashed lines reported in the figure. For InBi, these peaks are at $2\theta = 25.28°$ and 25.88°, and are due to the (110) and (101) planes, respectively; for In_2Bi, at 32.66° and 33.28° due to the (110) and (102) planes; and, finally, for In_5Bi_3, at 28.31° and 29.45° due to the (004) and (220) planes. In agreement with previous results, all three In–Bi com-

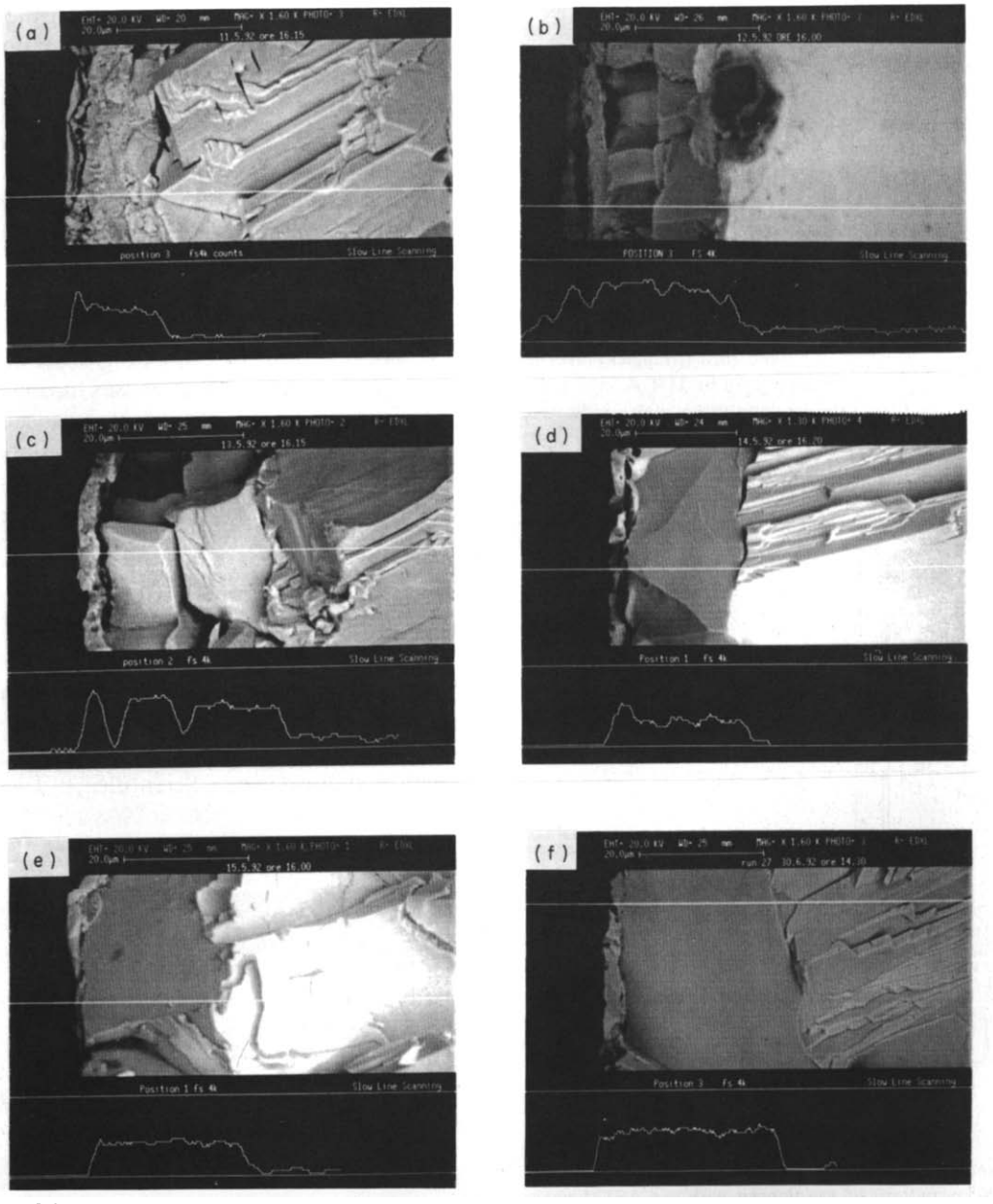

Fig. 5. SEM images of the cross-section of a deposit (a) 0.7 h, (b) 24.5 h, (c) 48.1 h, (d) 72.1 h, (e) 95.8 h and (f) 1193.2 h after electrodeposition at 21.4 A m^{-2} for 3 h. The In-line profile (scanned along the white line in the micrographs) is reported below.

pounds (in particular In_5Bi_3) are observed in Fig. 7, while Bi and In are scarcely visible.

To give further support to the SEM–EDS results, we also analysed the time evolution of the area of the characteristic diffraction peaks. In our semiquantitative evaluation, we neglected the X-ray absorption of the layers ahead of the considered intermetallic compound. These layers change both in thickness and composition, but composition changes are of minor importance, since the mass absorption coefficients of In and Bi for Cu Kα radiation are practically the same (252 and 253, respectively).

The results mimic those already discussed: i.e. the entire disappearance of In from the surface, the evolution of the two transient compounds In_2Bi and In_5Bi_3 (the latter disappearing before the former), and the continuous increase of the InBi layer.

4. Conclusions

The experimental results reported in this paper have confirmed those we previously obtained [1,2]. The latter showed that In electrodeposition from aqueous solutions on Bi cathodes, at 25 °C, easily diffuses into the substrate, so that the composition of the electrode surface depends on the current density. At medium to low current densities, the surface is coated by the InBi intermetallic

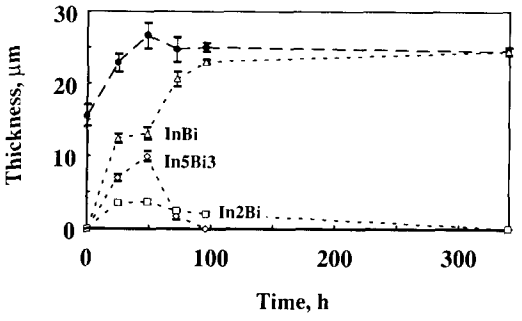

Fig. 6. Cumulative thickness of the deposit (dots) and thickness of the In_2Bi (squares). In_5Bi_3 (diamonds) and InBi (triangles) layer as a function of time after In electrodeposition at 21.4 A m^{-2} for 3 h. The standard deviation from the medium value is also indicated.

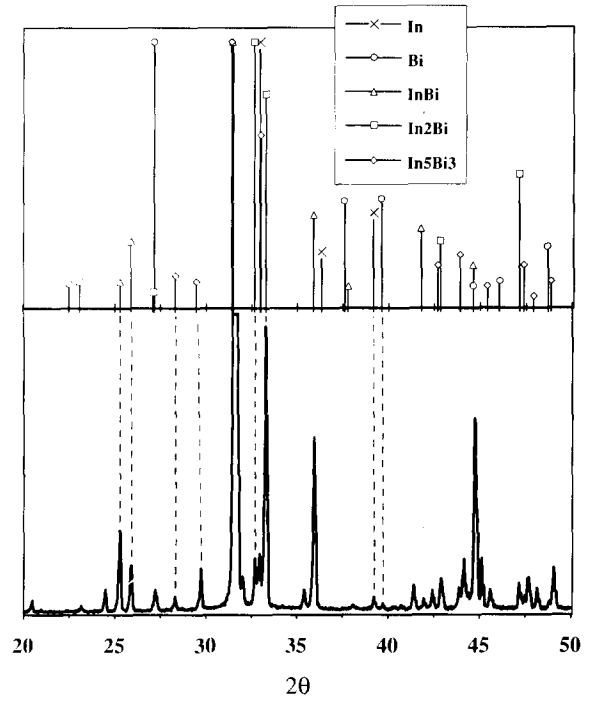

Fig. 7. Comparison 10 h after In electrodeposition (at 21.4 A m^{-2} for 3 h) of the X-ray pattern of the deposit with the ASTM peaks of In, Bi, InBi, In_2Bi and In_5Bi_3 [14]. The dashed lines connect the identification peaks of each metal or compound.

compound; at higher current densities, by In_2Bi; and, finally, at the highest current densities, by In. Such a phenomenology was previously described qualitatively.

Through a more accurate composition and structure investigation, the recent experiments have shown that the formation of the InBi phase on the electrode surface requires the formation of a third intermetallic compound (In_5Bi_3) separating InBi from In_2Bi.

This compound never emerges on the electrode surface: it appears exclusively as a separation phase.

The trend of the In diffusion and reaction process has been investigated after interruption of the circulating current, and we observed that such a process goes on until the whole electrodeposited In is bonded as InBi.

The experimental results are more complex than – but not in contrast with – those previously obtained [1,2], and allow one to understand the solid-state process of diffusion and reaction. The evolution of the system is similar to that occurring in other metallic systems (e.g. AlSb, AuSn, CdCu, FeZn) with the formation of overlayers of intermetallic phases having a narrow range of homogeneity [15]. The reaction proceeds by diffusion of the participating component/components through these layers, which separate the reactants from another and are ordered according to their relative composition.

Acknowledgments

This work is part of the Ph.D. thesis of S. Canegallo. V. Demeneopoulos is indebted to the Time (Erasmus) programme for a grant. The research was carried out with the financial support of the Ministero della Università e della Ricerca Scientifica e Tecnologica.

References

[1] L. Peraldo Bicelli, C. Romagnani and G. Serravalle, *Electrochim. Metal., IV. 3* (1969) 233.
[2] C. Sunseri and G. Serravalle, *Metall. Ital., 7/8* (1976) 373.
[3] V.M. Kochegarov and V.D. Samuilenkova, *Elektrokhimiya, 1* (1965) 1470.
[4] Y.N. Sadana and Z.Z. Wang, *Surf. Technol., 25* (1985) 17.
[5] Y.N. Sadana and Z.Z. Wang, *Met. Finish., 83* (1985) 23.
[6] V.V. Povetkin and T.G. Shibleva, *Zashch. Met., 29* (1993) 518; *Chemical Abstract, 119* (1993) 169253w.
[7] M.C. Hobson Jr. and H. Leidheiser Jr., *Trans. Met. Soc. AIME, 233* (1965) 482.
[8] R. Piontelli and G. Serravalle, *Electrochim. Metal., 1* (1966) 149; G. Serravalle, *Proc. Symp. on Sulfamic Acid,* Milan, 1966, Associazione Italiana di Metallurgia (AIM), Milan, p. 63.
[9] A.N. Campbell, *Can. J. Chem., 55* (1977) 1710.
[10] B.C. Giessen, A. Morris and N.J. Grant, *Trans. TMS AIME, 239* (1967) 883.
[11] O.H. Henry and E.L. Badwick, *Trans. AIME, 171* (1947) 389.
[12] E.A. Peretti and S.C. Carapella, *Trans. Am. Soc. Met., 41* (1949) 947.
[13] P.Y. Chevalier, *Calphad, 12* (1988) 383.
[14] *ASTM Cards: 5-0642,* 1974 (In); *5-0519,* 1974 (Bi); *32-113,* 1990 (InBi); *23-850,* 1983 (In_5Bi_3); *11-566,* 1972 (In_2Bi).
[15] H. Schmalzried, *Solid State Reactions,* Academic Press, New York, 1974, p. 124.